Optical Engineering

SPIEDigitalLibrary.org/oe

Achromatic triplet and athermalized lens assembly for both midwave and longwave infrared spectra

Chih-Wei Kuo

SPIE

Achromatic triplet and athermalized lens assembly for both midwave and longwave infrared spectra

Chih-Wei Kuo
National United University
Department of Electro-Optical Engineering
Miaoli 360, Taiwan
and
Chung-Shan Institute of Science & Technology
Electro-Optics Section
Materials & Electro-Optics Research Division
Lung-Tan 325, Taiwan
E-mail: kuocw00@yahoo.com.tw

Abstract. Analytic solutions for finding the achromatic triplet in the midwave and longwave infrared spectra simultaneously are explored. The relationship between the combination of promising refractive materials and the system's optical power is also formulated. The principles for stabilizing the effective focal length of an air-spaced lens group with respect to temperature are explored, and the thermal properties of the optical component and mechanical elements mutually counterbalanced. An optical design based on these achromatic and athermal theories is demonstrated, and the image quality of the lens assembly seems to approach the diffractive limitation. [DOI: 10.1117/1.OE.53.2.021102]

Subject terms: infrared; achromatic; athermal; dual band.

Paper 130263SS received Feb. 17, 2013; revised manuscript received Mar. 28, 2013; accepted for publication Apr. 11, 2013; published online Aug. 29, 2013.

1 Introduction

Thermal imaging technology, both midwave infrared (MWIR, wavelength from 3 to 5 μm) and longwave infrared (LWIR, wavelength from 8 to 12 μm) spectra have been extensively discussed in numerous studies over the past few decades.[1–4] Their applications cover a wide range of different fields, such as for industrial temperature measurement, noninvasive medical inspection, military stealth surveillance, and security biometrics recognition. Visual processing of these thermal images is commonly accomplished by utilizing the intensity threshold algorithm in which the intensities of the target pixels are compared with those of the background. Consequently, the difference in radiation between the target and the background has to exceed the threshold of the signal processing ability. However, unavoidable clutter and noise leads to deterioration in the contrast between the target and background in both the MWIR and LWIR spectra. The algorithm for temperature analysis in the multispectral infrared regions is explained,[5,6] making possible better target discrimination when the background is a similar temperature.

Over the past few years, the quantum well infrared photodetector (QWIP) and mercury cadmium telluride (MCT) detector technology has been developed. This has allowed for achieving pixel spatial registration and simultaneous output with a dual-band sensor. This system operates in both the MWIR and LWIR spectral region.[7] Such a dual-band sensor, with the assistance of the dual-band infrared color vision algorithm has the advantages of enhanced scenery awareness and effective image contrast within a single-color infrared camera.[8] Compared with the MCT, the QWIP possesses the disadvantage of lower quantum efficiency and a much lower cooling temperature.[9] On the other hand, QWIP with its advantages of higher yield and better uniformity from the III-V semiconductor manufacturing process, was accepted more easily for military and commercial applications.

There have been several papers documenting dual- and wide-spectral band optical system design[10–15] that have aimed at providing the chromatic correction over these wave bands by exploring the optical material combinations. Robert and Rogers selected candidate infrared refractive materials for use in the wide band range,[10] and designed an optical lens with a Petzval layout using a pair of triplets, but without the consideration of a cold shield. Jamieson derived the equations to correct for chromatic aberration with two and three refractive material combinations.[11] It was concluded that it was difficult to find a pair of refractive materials that meet the requirement for the ratio of index difference over the infrared wave bands. Furthermore, the relationship between three refractive materials to satisfy the chromatic problem could not guarantee that the optical power would be unified in different wave bands. Tamagawa and Tajime utilized a chart method to design the achromatized and athermalized optics for dual bands.[12] Its triplet objective was restricted by the rare material selection, and its field of view was inappropriate for the size of the focal plane array (FPA) in current QWIP or MCT devices. Wood and Roger explored the hybrid refractive-diffractive lenses for dual wave band infrared systems.[13] They called attention to the performance degradation caused by the unintended diffraction order, and the hybrid solutions that did not share a common focal plane at different wave bands. Vizgaitis demonstrated several optical designs dealing with refractive zoom and catadioptric zoom at the dual band spectrum.[14] Zhang et al. utilized the reimaged layouts for reducing pupil wander at the primary objective,[15] so the intermediate focal plane was relayed to the final FPA at the dual band region.

To ensure that the extreme S/N ratio is obtained, most infrared semiconductor detectors are cryogenically cooled. The whole radiometry detector unit (RDU) must be thermally insulated. A special aperture is located inside the RDU, known as the cold stop, and it causes the FPA to only receive remote scene radiation and the energy from the interior of the lens barrel. The optical system's aperture stop always coincides with the cold stop. This is necessary to avoid anomalous images and achieve 100% cold stop

efficiency.[16–18] Unlike the visible spectrum lens design, without the symmetrical principle to assist in eliminating partial aberrations, the stop shift cannot deal with balancing aberrations. Therefore, the cold stop restriction makes it harder than usual to come up with an infrared optical lens design.

The geometric dimensions and refractive index of the optical elements fluctuate with the variation in environmental temperature, and the focal length and wave aberrations are also affected accordingly.[19–21] The methodology for stabilizing the optical performance is named athermalization. This can be accomplished by either optomechanical mounting or optical compensation. The former is mostly concerned with eliminating the thermal defocus problem by the choice of the appropriate barrel dimensions and materials. Only first order aberrations are dealt with. The higher order aberrations lead to a continual deterioration in the image quality as the temperature change grows. The latter method is facilitated by basing each lens' power and differential index on the temperature and coefficient of thermal expansion during the optical design process, making a doublet or triplet without thermal defocus. In a practical layout, multiple doublets or triplets are composed to satisfy the requirements of the optical system. In the optical athermalization method, all the lens groups have to be taken into consideration.

2 Thin Lens Solution for an Achromatic Triplet at the Dual Band

Refractive optical systems are popular because they make both compact packaging and simplified alignment easier than when reflective or catadioptric systems are used. However, the refractive index of optical materials is a function of the wavelength. Excluding monochromatic applications, most optical systems are restricted to a waveband in which the chromatic aberrations are still tolerable.

The primary challenge of achromatic design for an optical system which would be suitable for both the MWIR and LWIR spectra simultaneously is the refractive material selection. There are not such abundant options for optical glass as exist in the visible spectrum due to the limitations of the transmittance property. The optical refractive material selection for MWIR and LWIR dual bands is significantly scaled down,[22] the major materials being only germanium (Ge), zinc sulfide (ZnS), zinc selenide (ZnSe), gallium arsenide (GaAs), and the other chalcogenide materials such as AMTIR. The most commonly used material for MWIR is silicon (Si) which cannot cover the full LWIR spectrum. Calcium fluoride (CaF_2) and barium fluoride (BaF_2) are candidates to be used from ultraviolet to infrared, but their lower refractive index makes it more difficult to eliminate spherical aberrations.

The achromatic triplet equations derived in this paper are similar to those for achromatic doublet and apochromatic triplet in a single bandwidth, except that dual separated bands are considered. These are essential for the initial optical design stage.

Let subscripts A and B represent the two reference wavelengths at the center of the separate dual bands, namely MWIR and LWIR. Now, select an arbitrary wavelength X that exists between A and B. The digital numbers in the subscripts indicate the different refractive materials. The triplet's optical power ϕ is composed of the summation of all the thin lens powers, and the optical powers operating in different wavebands are the same ($\phi = \phi_A = \phi_B$):

$$\phi_{1A} + \phi_{2A} + \phi_{3A} = \phi_A \tag{1}$$

$$\phi_{1B} + \phi_{2B} + \phi_{3B} = \phi_B. \tag{2}$$

The refractive index is a function of the wavelength. Each lens power can be expressed as a relationship between the dual bands with a specific coefficient, namely α, β, and

$$\phi_{1A} = \alpha\phi_{1B} \tag{3}$$

$$\phi_{2A} = \beta\phi_{2B} \tag{4}$$

$$\phi_{3A} = \gamma\phi_{3B}. \tag{5}$$

The Abbe number at wavelength X (known as ν_X) is defined by the reciprocal relative dispersion as follows:

$$\nu_X = \frac{n_X - 1}{n_A - n_B}. \tag{6}$$

The achromatic equation for wavelengths A (i.e., 4 μm) and B (i.e., 10 μm) in common focus is described by Eq. (7).[23] The ratio of optical power at wavelengths A and X (being k, l, and m for different materials), are listed in Eqs. (8), (9), and (10):

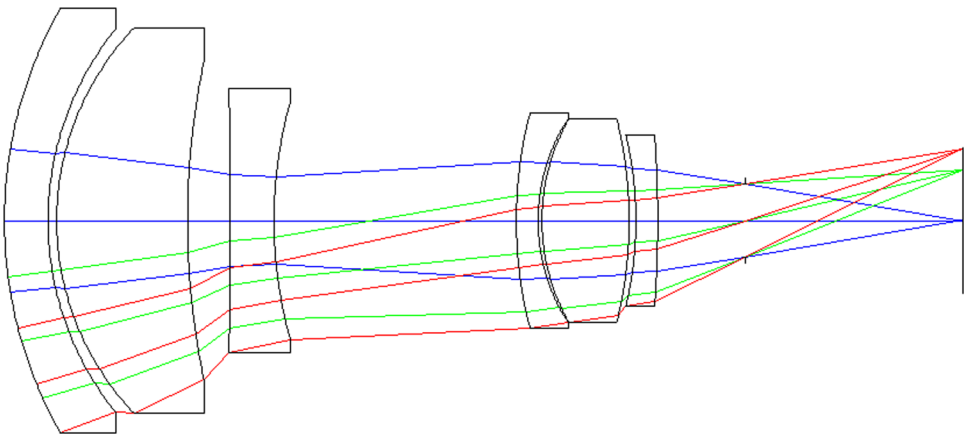

Fig. 1 Optical system layout.

Table 1 Lens prescription.

Surf	Radius	Thickness	Glass
1	49.57	5.00	ZNS
2	35.11	1.00	
3	32.00	15.00	ZNSE
4	88.16	4.94	
5	−650.71	5.00	GAAS
6	50.58	27.82	
7	49.54	2.50	ZNS
8	21.54	0.44	
9	23.49	10.00	ZNSE
10	−49.19	0.78	
11	−42.36	2.50	AMTIR1
12	−138.18	10.00	
STO	Infinity	25.00	
IMA	Infinity		

$$\frac{\phi_{1X}}{\nu_{1X}}+\frac{\phi_{2X}}{\nu_{2X}}+\frac{\phi_{3X}}{\nu_{3X}}=0 \tag{7}$$

$$\phi_{1X}=k\phi_{1A} \tag{8}$$

$$\phi_{2X}=l\phi_{2A} \tag{9}$$

$$\phi_{3X}=m\phi_{3A}. \tag{10}$$

The symbol of ϕ_A in Eq. (1) is replaced by ϕ to result in Eq. (11). Equations (3), (4), and (5) are substituted into Eq. (2), and Eq. (12) is formulated. Then, Eq. (13) is derived by substituting Eqs. (8), (9), and (10) into Eq. (7). We derived three linear algebraic equations as follows:

$$\phi_{1A}+\phi_{2A}+\phi_{3A}=\phi, \tag{11}$$

$$\left(\frac{1}{\alpha}\right)\varphi_{1A}+\left(\frac{1}{\beta}\right)\varphi_{2A}+\left(\frac{1}{\gamma}\right)\varphi_{3A}=\varphi, \tag{12}$$

$$\left(\frac{k}{\nu_{1X}}\right)\varphi_{1A}+\left(\frac{l}{\nu_{2X}}\right)\varphi_{2A}+\left(\frac{m}{\nu_{3X}}\right)\varphi_{3A}=0. \tag{13}$$

The above solution for the three unknowns, ϕ_{1A}, ϕ_{2A}, and ϕ_{3A}, can be calculated by Cramer's rule from Eqs. (11) to (13).

For example, a triplet optical power ϕ (=0.033333) is required, and wavelength A (=4 μm), X (=7 μm), and B (=10 μm) are set. We choose ZnS, ZnSe, and AMTIR1 as lens materials accordingly, and the constants α (=1.043803), β (=1.019), γ (=1.011315), k (=0.983551), l (=0.992081), and m (=0.994612) are acquired. Abbe numbers are ν_{1X} (=23.437621), ν_{2X} (=53.20806), ν_{3X} (=88.897965). Substituting these numbers into Eqs. (11) to (13), the optical power of each lens, ϕ_1 (= − 0.0073), ϕ_2 (= − 0.0201), and ϕ_3 (=0.0607), are calculated.

3 Athermalization for a Pair of Air-Spaced Achromatic Triplets

Jamieson discussed the process of athermalization for doublets and triplets with analytical methods, for an optical system composed only of either a doublet or triplet.[21] It was implied that the effective focal length and barrel length were equal. However, most of the practical configurations were compound of air-spaced lens groups, such as in

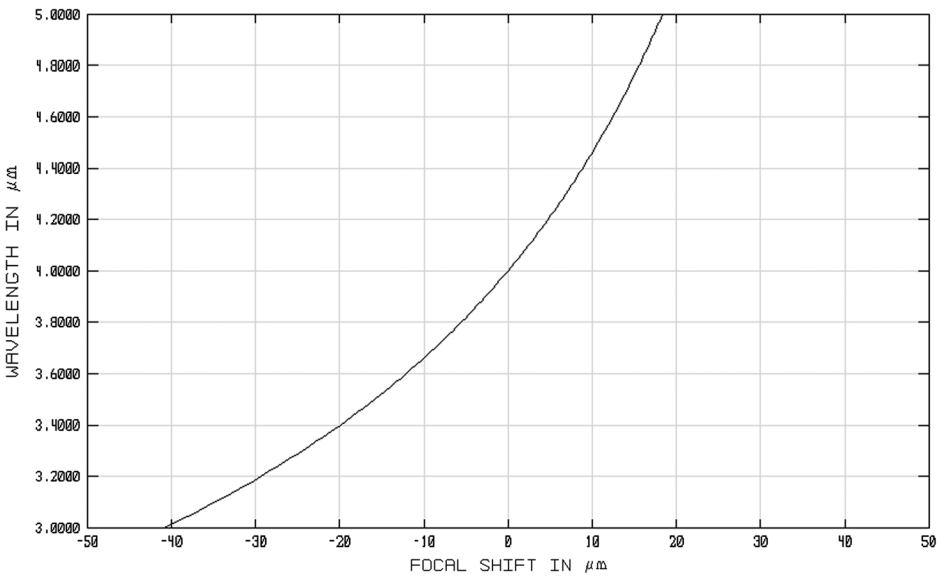

Fig. 2 Chromatic focal shift of MWIR.

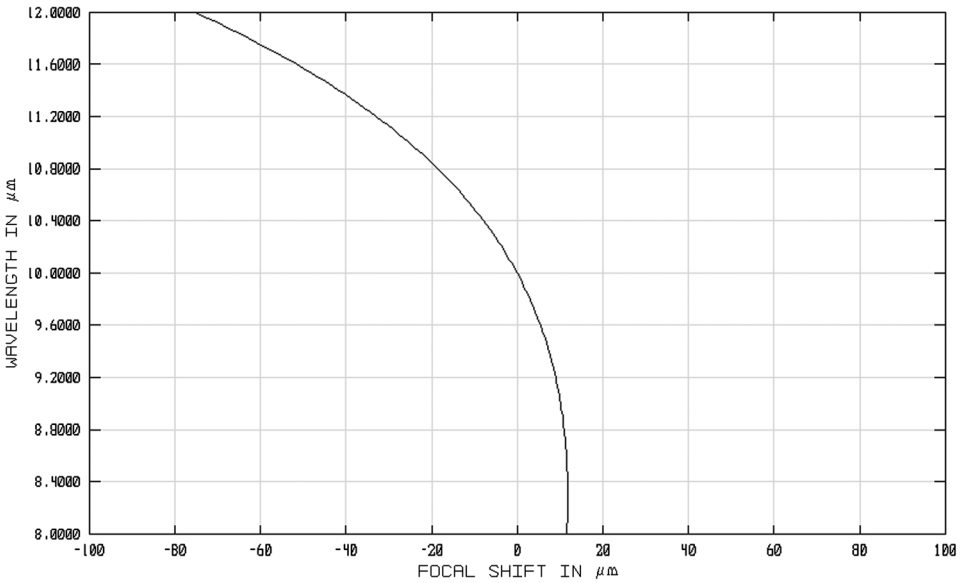

Fig. 3 Chromatic focal shift of LWIR.

telephoto and reverse-telephoto layouts. Jamieson also proposed a wave aberration method to evaluate the change of focal length caused by each lens in a multiple lens system.[21] It did not take into account the thermal expansion of the barrel, and it needed the paraxial ray height at each lens for calculating the wave aberration change due to thermal defocus, which made the initial layout more difficult.

This paper presents the analytical equations for designing athermalized air-spaced lens assemblies. By employing a pair of separated lens groups, which could be achromatic triplets at dual bands as described in the above section, we find the optical power of the system ϕ as follows:

$$\phi = \phi_F + \phi_R - S\phi_F\phi_R, \tag{14}$$

where subscript F as well as R represent the optical power of the front and rear lens group, respectively; and S is the distance of the principle plane between the front and rear lens groups. This equation is differentiated with respect to temperature T and rearranged as

$$\frac{\mathrm{d}\phi}{\mathrm{d}T} = \phi_F\delta_F + \phi_R\delta_R - S\phi_F\phi_R(\delta_F + \delta_R + \theta), \tag{15}$$

$$\delta = \frac{\left(\frac{\mathrm{d}\phi}{\mathrm{d}T}\right)}{\phi}, \tag{16}$$

$$\theta = \frac{\left(\frac{\mathrm{d}S}{\mathrm{d}T}\right)}{S}, \tag{17}$$

where δ is the coefficient of thermal optics (CTO) of the lens material; and θ is the coefficient of thermal expansion (CTE) of the barrel's material. The coefficient of thermal optics has also been referred to by some authors as the thermal defocus

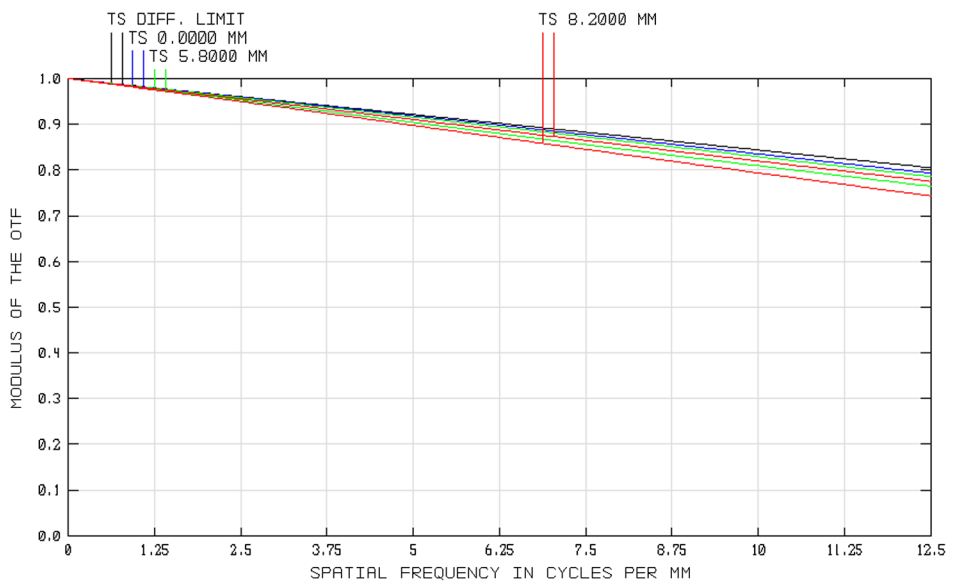

Fig. 4 MTF of MWIR.

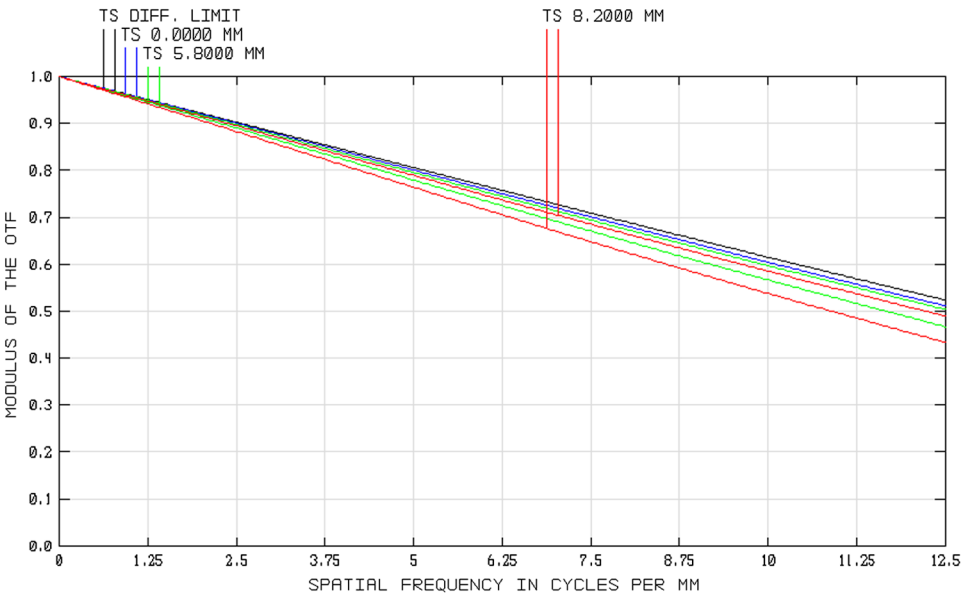

Fig. 5 MTF of LWIR.

coefficient[19] or thermal dispersive power.[12] The CTO depends less on the wavelength than the optical power does. Its difference with changes in the wavelength can be neglected if the mean value of CTO covering the dual bands is introduced.[12] Therefore, the mean value of CTO is effective in the initial design stage.

To meet the athermalization requirement, the optical power differentiation with respect to temperature is set to zero. Then, the mathematical solution of CTE could be easily solved from Eqs. (14) and (15):

$$\theta = \left[\frac{(\phi_F\delta_F + \phi_R\delta_R)}{(S\delta_F\delta_R)} - (\delta_F + \delta_R)\right] = \left\{\frac{(\phi_F\delta_F + \phi_R\delta_R)}{[(\delta_F + \delta_R) - \phi]} - (\delta_F + \delta_R)\right\}. \quad (18)$$

However, the mathematical solution does not always match the physical CTE corresponding to the material selected for the barrel. A bi-metal combination layout could offer an alternative, and the apparent CTE is synthesized by

$$\theta = \frac{(\theta_1 S_1 + \theta_2 S_2)}{(S_1 + S_2)}, \quad (19)$$

$$S = S_1 + S_2, \quad (20)$$

where the subscript number represents the different metal material selected. In practical applications, the optical power changes with temperature compared with the optical power, i.e., thermal dispersive power (δ), being relatively small, facilitating athermalization. Consequently, a system with a greater effective focal length is more vulnerable to temperature change.

4 Optical Design and Optimization

In this study, the optical system design is assigned specifications of relative aperture or speed (F/3), effective focal length (EFL = 50 mm), and a greater back focal length (BFL > 30 mm) for accommodating the cold shield distance. A quantum well infrared photodetector sensor was used in this study, which operated at MWIR and LWIR dual-bands infrared spectrum. The QWIP focal plane array had a 320×256 pixel number and 40 μm squared pixel size. The aperture stop coincided with the cold stop for eliminating anomalous images.

The refractive material of the lens was set accordingly, by utilizing the thin lens solution for an achromatic triplet at the dual band. The primary candidate materials were germanium (Ge), zinc sulfide (ZnS), zinc selenide (ZnSe), gallium arsenide (GaAs), and the chalcogenide material (AMTIR1). There were a lot of combinations for the achromatic triplet, but the solutions leading to greater optical power were not recommended for the reason of reducing the aberration. A negative achromatic triplet and a positive one were thus composed, and the reverse telephoto layout was constructed. The initial

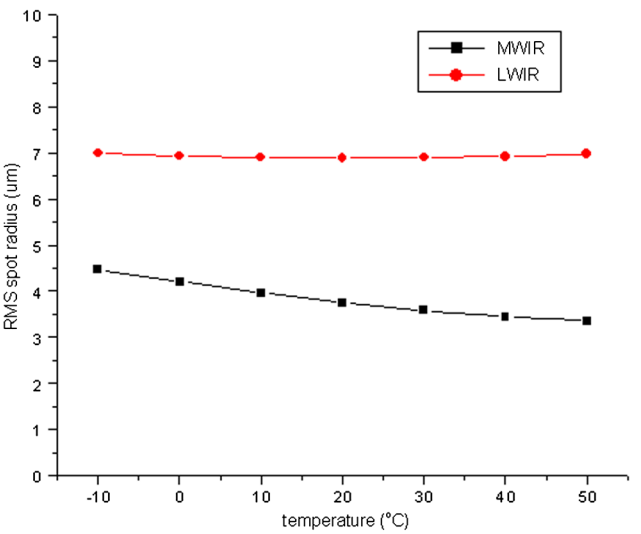

Fig. 6 The on-axis RMS spot radius of MWIR and LWIR.

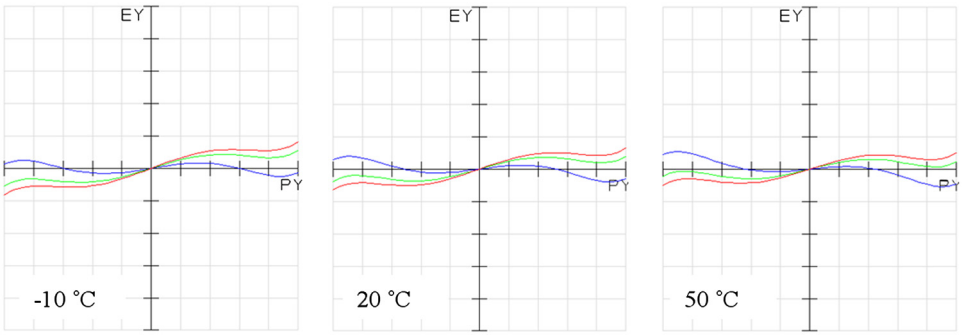

Fig. 7 Axial transverse ray aberrations of MWIR (plot scale ± 50 μm).

design was tested by trial and error to satisfy the achromatic and athermalization requirements.

The final aberrations were evaluated and optimized with the ZEMAX commercial software. The weighting functions of the FOV were set equally at the on-axis, 0.707, and at the full FOV. The MWIR spectra (3, 4, and 5 μm) and LWIR spectra (8, 10, and 12 μm) were defined using the multi-configuration with the uniform weighting functions. The damped least square algorithm is used to calculate the merit function (MF)

$$\mathrm{MF} = \sum_{j=1}^{N} W_j (V_j - T_j)^2, \tag{21}$$

where W is the weighting function; V is the current value; and T is the target value. The subscript represents the operand item number. At the beginning of optimization, the RMS spot radius was taken as a merit function. At the final stage of optimization, the wavefront error was taken as the system performance approached the diffraction limits. The reverse telephoto design assembled from a pair of achromatic triplet combinations is shown in Fig. 1.

The total length from the first surface to FPA was less than 110 mm, and the back focal length was greater than 30 mm. The aperture stop coincided with the cold shield, so the most forward lens had a maximum diameter of less than 50 mm. There was no vignetting and the real image height covered the diagonal size of FPA. The final lens design prescription is given in Table 1.

The chromatic focal shifts of the MWIR as well as LWIR are listed in Figs. 2 and 3, respectively. The ordinate represents the wavelength and the abscissa describes the focal shift. The curves show no focal shift at the center wavelength of both 4 and 10 μm for the dual bands. The maximum focal shift range of either MWIR or LWIR is less than the depth of focus setting obtained by using the Rayleigh's quarter-wave criterion, i.e., $\pm 2\lambda(F/)^2$. This implies that the residual longitudinal chromatic aberration is still inside the tolerable allowance.

The dual band MTFs are also plotted individually in Figs. 4 and 5. For both the MWIR and LWIR spectra, the lens image quality is pushed toward the diffractive limitation. The MTF curve of MWIR shows higher modulation than that of the LWIR at the same frequency for the shorter wavelength producing better spatial resolution. From the sampling theorem for the FPA pixel size, the image frequencies greater than the Nyquist limitation were aliased, and the MTF curve was truncated there.

First, this optical system was designed for a default temperature of 20°C. To evaluate the design and obtain athermalization results, several environmental temperatures ($T = -10$°C, 0°C, 10°C, 20°C, 30°C, 40°C, and 50°C) were simulated. An aluminum alloy was utilized for the barrel. A plot of the dual band's on-axis RMS spot radius versus temperature is shown in Fig. 6. The curves show that the radius size did not significantly change with temperature. The radii of the airy disks for MWIR and LWIR were 14.81 and 36.98 μm, respectively, and the spot diagram from geometrical ray tracing did not exceed these values. It can be seen that the geometrical aberrations were significantly smaller than the diffraction blur. The image quality of this optical design was still dominated by the diffractive theory without apparent temperature effects. The axial transverse ray aberrations of this athermalized design at temperatures of −10°C, 20°C, and 50°C are listed in Figs. 7 and 8

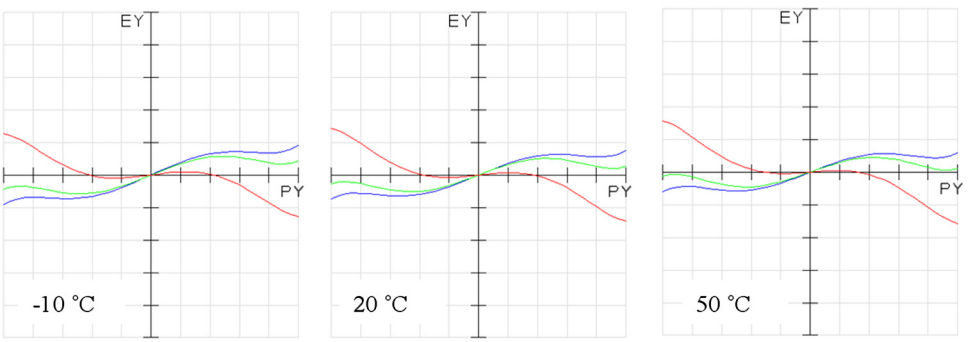

Fig. 8 Axial transverse ray aberrations of LWIR (plot scale ± 50 μm).

(for MWIR and LWIR, respectively). It can be seen that there are quite small variations (plot scale $\pm$ 50 μm).

5 Conclusion

This paper introduces a method for solving the achromatic triplet analytic solution for MWIR and LWIR simultaneously, as well as mentioning the refractive materials. An analytic equation for designing athermalized air-spaced lens assemblies without the necessity of ray tracing at each surface is also discussed. A reverse telephoto setup composed of a pair of achromatic triplets is designed and optimized. This lens assembly demonstrated both achromatic and athermal results with image quality approaching the diffractive limit for MWIR and LWIR simultaneously.

Acknowledgments

The author is grateful for the discussion and contribution of his colleagues in the EO Section, Materials and Electro-Optics Research Division, Chung-Shan Institute of Science and Technology, and faculty members in the Department of Electro-Optical Engineering, National United University.

References

1. C. W. Kuo, C. L. Lin, and C. Y. Han, "Dual field-of-view midwave infrared optical design and athermalization analysis," *Appl. Opt.* **49**(19), 3691–3700 (2010).
2. C. W. Kuo, J. M. Miao, and C. H. Tai, "Midwave infrared optical zooming design and kinoform degrading evaluation methods," *Appl. Opt.* **50**(18), 3043–3049 (2011).
3. R. E. Fischer and T. U. Kampe, "Actively controlled 5:1 afocal zoom attachment for common module FLIR," *Proc. SPIE* **1690**, 137–152 (1992).
4. J. I. Kudo et al., "Diffractive lens in 8- to 10-μm forward-looking infrared system," *Opt. Eng.* **41**(8), 1787–1791 (2002).
5. M. J. Duggin, "Discrimination of targets from background of similar temperature, using two-channel data in the 3.5-4.1-um and 11–12-um regions," *Appl. Opt.* **25**(7), 1186–1195 (1986).
6. M. H. Horman, "Temperature analysis from multispectral infrared data," *Appl. Opt.* **15**(9), 2099–2104 (1976).
7. A. Goldberg, T. Fischer, and S. Kennerly, "Dual band QWIP MWIR/LWIR focal plane array test results," *Proc. SPIE* **4028**, 276–287 (2000).
8. D. Scribner et al., "Infrared color vision: separating objects from backgrounds," *Proc. SPIE* **3379**, 2–13 (1998).
9. H. K. Pollehn and J. Ahearn, "Multi-domail smart sensors," *Proc. SPIE* **3698**, 420–426 (1999).
10. M. Roberts and P. J. Rogers, "Wide waveband infrared optics," *Proc. SPIE* **1013**, 84–91 (1988).
11. T. H. Jamieson, "Ultrawide waveband optics," *Opt. Eng.* **23**(2), 111–116 (1984).
12. Y. Tamagawa and T. Tajime, "Dual-band optical systems with a projective athermal chart: design," *Appl. Opt.* **36**(1), 297–301 (1997).
13. A. P. Wood and P. J. Roger, "Hybrid optics in dual waveband infrared system," *Proc. SPIE* **3482**, 602–618 (1998).
14. J. N. Vizgaitis, "Optical concepts for dual band infrared continuous zoom lenses," *Proc. SPIE* **7652**, 76522E (2010).
15. Y. C. Zhang et al., "Mid and long waveband infrared imaging system design," *Proc. SPIE* **7494**, 74940M (2009).
16. M. N. Akram, "Design of a dual field-of-view optical system for infrared focal plane arrays," *Proc. SPIE* **4768**, 10–20 (2002).
17. C. W. Kuo, "Scene-based nonuniformity correction midwave infrared staring array triple field of view lens design," *Opt. Eng.* **51**(10), 103001 (2012).
18. R. E. Fischer and B. Tadic-Galeb, *Optical System Design*, pp. 223–226, McGraw-Hill, New York (2000).
19. P. R. Yoder, "Effects of temperature changes on optical component mountings," Chap. 12 in *Mounting Optics in Optical Instruments*, SPIE, Bellingham, Washington (2002).
20. D. Vukobratovich, "Optomechanical systems design," Chap. 3 in *The Infrared & Electro-Optical Systems Handbook*, Vol. 4, ERIM, SPIE, Bellingham, Washington (1993).
21. T. H. Jamieson, "Athermalization of optical instruments from the optomechanical viewpoint," *Optomechanical Design* **CR43**, pp. 131–159, SPIE, Bellingham, WA (1992).
22. J. N. Vizgaitis, "Third generation infrared optics," *Proc. SPIE* **6940**, 69400S (2008).
23. J. M. Geary, *Introduction to Lens Design with Practical ZEMAX Examples*, p. 229, Willmann-Bell, Richmond, Virginia (2002).

Chih-Wei Kuo received his bachelor's degree in mechanical engineering from National Central University, in 1991. He received master's degree in mechanical engineering from National Taiwan University, in 1993. He worked for Electro-Optics Section of CSIST in 1997, and he received PhD in mechanical engineering from National Central University, in 2006. His research interests are imaging lens design, optomechanical structure analysis, digital image processing, and non-imaging optical modeling.